Fluid-Structure Interaction and High-Performance Computing to serve sport performance in rowing

A. Leroyer[a], S. Barré[b], G.B. Deng[c], J. Wackers [d], E. Guilmineau [e], M. Visonneau [f], P. Queutey [g]

a. LHEEA, UMR-CNRS 6598, Centrale Nantes, alban.leroyer@ec-nantes.fr
b. CREPS Pays-de-la-Loire, sophie.barre@creps-pdl.sports.gouv.fr
c. LHEEA, UMR-CNRS 6598, Centrale Nantes, ganbo.deng@ec-nantes.fr
d. LHEEA, UMR-CNRS 6598, Centrale Nantes, jeroen.wackers@ec-nantes.fr
e. LHEEA, UMR-CNRS 6598, Centrale Nantes, emmanuel.guilmineau@ec-nantes.fr
f. LHEEA, UMR-CNRS 6598, Centrale Nantes, michel.visonneau@ec-nantes.fr
g. LHEEA, UMR-CNRS 6598, Centrale Nantes, patrick.queutey@ec-nantes.fr

Résumé :

L'augmentation considérable de la puissance de calculs des ordinateurs permet aujourd'hui à la simulation numérique de se positionner en tant qu'outil d'analyse et aide à la performance sportive. Cependant, la tâche s'avère souvent tout de même ambitieuse et ardue pour les raisons suivantes : les configurations physiques mise en jeu impliquent une approche pluridisciplinaire où l'humain fait partie intégrante du système étudié et interagit avec celui-ci. De plus, une exigence particulière est requise du fait que les athlètes élites sont déjà proches de l'optimum. Par conséquent, les modélisations des phénomèmes qui rentrent en jeu doivent fournir un degré de précision suffisant pour être utiles et pertinentes lorsqu'il s'agit de d'analyser des interactions complexes et de fournir des tendances fiables à des petites variations de paramètres. Le cas de l'aviron est présenté ici, au travers du développement d'un simulateur haute-fidélité du système global "bateau-avirons-rameur(s)", couplé avec la résolution des équations de Navier-Stokes pour fournir les efforts fluides agissant sur celui-ci. Pour ce sport nautique, ce sont les écoulements autour de la coque et des palettes très singuliers dans le monde de l'hydrodynamique navale associés aux interactions avec le système global dû aux mouvements du rameur et à la flexibité du manche qui font que cette démarche relève encore du défi scientifique.

Abstract :

With the tremendous growth of computational power, the use of numerical simulations to help analysing and improving sport performance becomes achievable but is still challenging because the physical configurations generally involved coupled problems and because a human is part of the system. Futhermore, elite athletes already operate near an optimal point. As a consequence, the modelization of all the phenomena that come into play has to be accurate enough to be useful and relevant when the objective is to analyse interactions and to give reliable trends while varying some parameters. The case of rowing is presented here, through the development of a high-fidelity simulator of the global system "boat-oars-rower(s)" coupled with the resolution of the Navier-Stokes equations to provide fluid forces acting on it. For this nautical sport, the complexity comes from the non-classical naval hydrodynamics flows around the hull and the blades and from the fluid-structure interactions with the global system due to the motion of the rower and the flexibility of the shaft.

Keywords : Fluid-Structure Interaction, Computational Fluid Dynamics, rowing simulator, sport performance

1   Introduction

Numerical simulations which require High-Performance Computing (HPC) are more and more used in all the fields of industry, yielding performance improvement for numerous products. This trend is similar in sports, especially when material and technology are involved. Numerical simulations become useful tools as performance aids : from weather forecast to estimate snow quality on the skiing track to use the best possible wax to Formula One racing car for which a lot of optimization (aerodynamics, structure, combustion...) are carried out thanks to great power computer. Nautical sports are not left behind, especially in sailing, where the design workflow is similar to the one used in the industry, since some of classes can afford skills, tools and computer power, as for the America's cup. A sport like rowing do not benefit from such a financial support. In addition to that, from the hydrodynamic point of view, it has some specificities which make it challenging : the athlete who is the propulsive machine has a great interaction with the system and uses blades which generate a violent unsteady flow near the free surface. The unsteadiness of the propulsion associated to the motion of the athlete with respect to his hull leads to large secondary motions, which are a singular feature for the flow around hulls in calm water in hydrodynamics. Another fluid-structure interaction (FSI) which influences the response of the global system boat-rower(s)-oar(s) is due to the flexibility of the oar shaft.

Previous research works have been done about the validation of the flow around the hull and around the blade ([20, 22]). Here, a focus is done on a recent work aiming at developing a high-fidelity modelling of the complete boat-oars-rower(s) system. This development has started with the contribution of a group of engineering students who followed the project-based specialisation named "Paris Scientifiques 2024/ Scientific Challenge 2024" at Centrale Nantes. To achieve this scientific challenge, a multibody system is developed to accurately model the kinematics of the rower with respect to its environment. This imposed kinematics is driven both by some gesture parameters and in-situ data measurements as the time evolution of the sweep angle of each oar. The dynamics of the global system is then reduced to the dynamics of the hull, which is solved by integrating the major fluid forces acting on both the hull and the blades through Computational Fluid Dynamics (CFD). This is done by coupling the Navier-Stokes solver ISIS-CFD developed by the METHRIC team at the LHEEA Lab. with a dedicated Python program which models the multibody system boat-oars-rower(s). Such a CFD configuration brings into play advanced numerical techniques such as the combined use of overset grid technique and adaptive grid refinement (AGR) ([29]). To reach an efficient and robust algorithm for this partionned approach, the coupling iteration occurs during the non-linear iterations of the fluid solver because it is the most costly part. This implicit internal coupling solves both the dynamics of the hull and the flexibility of the oar shafts. Data transfer between the two codes is done through a TCP socket by the way of the ZeroMQ library ([1]). As other fluid-structure interaction in hydrodynamics, a stabilization procedure based on an artificial added mass method is used to tackle the destabilising added-mass effects ([33]).

2   Modelling of the global system boat-oar(s)-rower(s)

Several works aiming at modelling the global system boat-oar(s)-rower(s) are found in the literature. Many of them consider the rower as a point mass whose motion is prescribed with respect to the boat

[4–6, 16, 17, 25, 27, 28]. Among them, a multi-body model is sometimes used, but only to refine the kinematics of the rower and then the evolution of the mass center position : the dynamics remain mass point based, with more or less refinement [5, 6, 16]. The analysis is then restricted to the interaction with the surge motion of the hull, without any consideration of pitch and heave motion and using simplified model for the fluid forces acting on the hull and on the blade. Only [27, 28] uses CFD to evaluation the fluid force acting on the blade with a point mass system, but without any vertical motion of the blade. Furthermore, the flexibility of the shaft taking into account in [27] seems to give strange results with a propulsive force negative at the end of the drive phase.

In contrast, [8, 9, 23, 24, 26] used more advanced multi-body model and take into account the evolution of the centre of mass and that of the inertia. A more realistic dynamics of the system can then be solved, by coupling the resolution of surge, heave and pitch motions. However, fluid model are again restricted to simplified model for the fluid force acting on the blade and more often for the hull too. Only [8, 9] used a potential flow to investigate the fluid force on the hull.

The present work aims at achieving such a complete model but using a fully coupling with a CFD solver to achieve fluid forces as accurate as possible. In addition to the design of a refine mechanical model for the global system, the primal objective is definitively oriented to be used in collaboration with the technical staff. As a consequence, instead of driving each join of the rower (by imposing kinematics or torque) and to deduce the evolution of the sweep angle in time as it is commonly done in the previous works, it was decided to base the control of the rower on this data. Actually, the sweep angle is the information which is accurately and daily measured in practise. Then, real kinematics can be easier be reproduced and analysed.

The GMRS solver ([23, 24]), which solves the dynamics of the global system using a robotic approach could have been used as a starting point. But the Matlab language associated to the complexity of the robotic approach for non-expert makes hard the pursuit of the development, the change of the control paradigm, the maintenance and the coupling with a CFD solver. Another option could have been to use some existing general purpose multi-body solvers like MBDyn already coupled in the past with the CFD code ([32]). But, the requirement specifications in term of driving through the sweep angle with some additional judicious parameters to charactize the technical gesture makes such a sophisticated tool not so appropriate. Finally, it was decided to develop a dedicated tool (named SPRing for "Simulator of Performance in Rowing") to have more freedom about the description of the technical gesture of the rower, and about the parameters which drive the rower motion, see section 4.2.

2.1   Parameterization of the multi-body system

Let define $\mathcal{R}_0 = (O_0, \mathcal{B}_0 = (\overrightarrow{x_0}, \overrightarrow{y_0}, \overrightarrow{z_0}))$ the Galilean frame of reference fixed to the Earth. A reference frame fixed to the boat is defined. The reference point of the system is arbitrarily set on the keel line at the middle of the boat, see figure 1. The orientation of $\mathcal{B}_b$ is supposed to be identical to $\mathcal{B}_0$ at the initial state.

The goal is finally to compute the relative position of $\mathcal{R}_b$ with respect to $\mathcal{R}_0$, by solving the Newton's law of the global system boat-oar(s)-rower(s), see section 2.2. The parameterization of $\mathcal{R}_b$ with respect to $\mathcal{R}_0$ is set through the coordinates of the vector $\overrightarrow{O_0 O_b}$ expressed in β_0, whereas the orientation is specified through the three classical successive rotations Yaw-Pitch-Roll (see figure 2).

Contrary to what is done in the generic Newton's law module implemented into the CFD solver ISIS-CFD, quaternions are not used here to parameterize the orientation. Since the configuration investigated
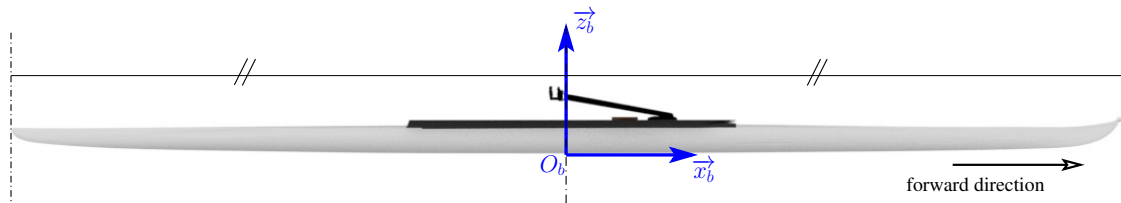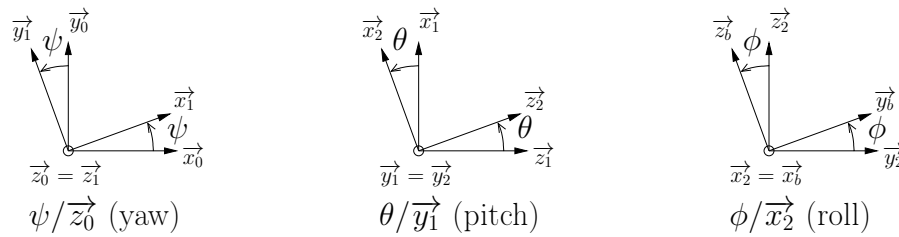
FIGURE 1 – Definition of the frame of reference for the boat

FIGURE 2 – Parameterization of the orientation ($\beta_b = \beta_3$)

here is not as general as the ISIS-CFD body dynamics module, it was decided to switch to the Cardan angles. Unless you want to replay the sinking of the Titanic, the problem of gimbal lock which appears when the pitch angle reaches 90 degree will never happer for the case of a rowing boat. In addition to that, the Cardan angles are more direct to interpret and give the possibility to easily imposed of fixed some rotation as the roll or the yaw, which are not the high-priority degree of freedom to investigate for the global dynamics of the considered system.

2.2 Resolution of the dynamics

The global system composed of a series of rigid bodies linked together can be considered as a particular case of a flexible body already studied in [10, 11]. A floating frame is also used and corresponds in the present case to the boat frame $\mathcal{R}_b$. The equations which describes the dynamics of the boat can be written as the equations (1) and (2).

$$\left.\frac{d\overrightarrow{V(O_b/\mathcal{R}_0)}}{dt}\right|_{\mathcal{R}_0} + \left.\frac{d\overrightarrow{\Omega_0^b}}{dt}\right|_{\mathcal{R}_0} \wedge \overrightarrow{O_bG} = \frac{\overrightarrow{\mathcal{T}}}{M_S} - \frac{\overrightarrow{\mathcal{S}_{Res}}}{M_S} \tag{1}$$

$$\text{with} \quad \frac{\overrightarrow{\mathcal{S}_{Res}}}{M_S} = \left.\frac{d\overrightarrow{V(G,S/\mathcal{R}_b)}}{dt}\right|_{\mathcal{R}_b} + 2\,\overrightarrow{\Omega_0^b} \wedge \overrightarrow{V(G,S/\mathcal{R}_b)} + \overrightarrow{\Omega_0^b} \wedge \left(\overrightarrow{\Omega_0^b} \wedge \overrightarrow{O_bG}\right)$$

$$M_S\overrightarrow{O_bG} \wedge \left.\frac{d\overrightarrow{V(O_b/\mathcal{R}_0)}}{dt}\right|_{\mathcal{R}_0} + \mathbb{I}(O_b,S)\left.\frac{d\overrightarrow{\Omega_0^b}}{dt}\right|_{\mathcal{R}_0} = \overrightarrow{\mathcal{M}}_{O_b} - \overrightarrow{\mathcal{S}_I} - \overrightarrow{\mathcal{S}_{Mom}} \tag{2}$$

$$\text{with} \qquad \overrightarrow{\mathcal{S}_I} = \iiint_S \rho_S \left(\overrightarrow{O_bM} \cdot \overrightarrow{\Omega_0^b} \right) \left(\overrightarrow{O_bM} \wedge \overrightarrow{\Omega_0^b} \right) dv$$

$$\overrightarrow{\mathcal{S}_{Mom}} = \left. \frac{d}{dt} \right|_{\mathcal{R}_b} \iiint_S \overrightarrow{O_bM} \wedge \rho_S \overrightarrow{V(M, S/\mathcal{R}_b)} \, dv$$

$$+ 2 \iiint_S \rho_S \left(\overrightarrow{V(M, S/\mathcal{R}_b)} \cdot \overrightarrow{O_bM} \right) \overrightarrow{\Omega_0^b} \, dv$$

$$- 2 \iiint_S \rho_S \left(\overrightarrow{O_bM} \cdot \overrightarrow{\Omega_0^b} \right) \overrightarrow{V(M, S/\mathcal{R}_b)} \, dv$$

where we define :

— G, M_S and $\mathbb{I}(O_b, S)$ the centre of mass of the global system S, its mass, and its inertia matrix expressed at the point O_b, respectively,

— $\overrightarrow{\Omega_0^b}$ the instantaneous rotation vector of β_b with respect to β_0,

— $\overrightarrow{\mathcal{T}}$ and $\overrightarrow{\mathcal{M}_{O_b}}$ the resultant and the moment at the point O_b of the external forces acting on the system (gravity, fluid force acting on the hull and on the blades, aerodynamic forces).

— $\overrightarrow{V(M, S/\mathcal{R}_b)}$ the velocity of a point M belonging to S with respect to $\mathcal{R}_b$,

— ρ_S the local density of the system S

However, contrary to what is done in [11], there is no need of a structure mesh to compute the inertial term $\overrightarrow{\mathcal{S}_{Mom}}$ here, since it can be directly computed taking advantage of this specific system composed of n rigid bodies denoted S_i, with mass M_i, centre of mass G_i and inertia $\mathbb{I}(G_i, S_i)$. If (A_i, B_i, C_i) and (D_i, E_i, F_i) mean the moments and the products of inertia as defined by equation (3), it can be deduced after some algebraic manipulations the expression of $\overrightarrow{\mathcal{S}_{Mom}}$ as defined by equation (4).

$$\mathbb{I}(G_i, S_i)|_{\mathcal{R}_b} = \begin{bmatrix} A_i & -F_i & -E_i \\ -F_i & B_i & -D_i \\ -E_i & -D_i & C_i \end{bmatrix} \tag{3}$$

$$\overrightarrow{\mathcal{S}_{Mom}} = M_i \sum_{i=1}^n \overrightarrow{O_bG_i} \wedge \overrightarrow{A(G_i, S_i/\mathcal{R}_b)} + \sum_{i=1}^n \left. \frac{d}{dt} \right|_{\mathcal{R}_b} \left(\mathbb{I}(G_i, S_i) \overrightarrow{\Omega_b^i} \right)$$

$$+ 2 M_i \sum_{i=1}^n \left(\overrightarrow{O_bG_i} \cdot \overrightarrow{V(G_i, S_i/\mathcal{R}_b)} \right) \cdot \overrightarrow{\Omega_0^b} \tag{4}$$

$$- 2 M_i \sum_{i=1}^n \left(\overrightarrow{O_bG_i} \cdot \overrightarrow{\Omega_0^b} \right) \overrightarrow{V(G_i, S_i/\mathcal{R}_b)} - 2 \sum_{i=1}^n \overrightarrow{\mathcal{S}_{MomIi}}$$

with

$$\overrightarrow{\mathcal{S}_{MomIi}} \cdot \overrightarrow{x_b} = \alpha\beta_i E_i - \alpha\gamma_i F_i + \beta\beta_i D_i - \beta\gamma_i \left(\frac{A_i + C_i - B_i}{2} \right) + \gamma\beta_i \left(\frac{A_i + B_i - C_i}{2} \right) - \gamma\gamma_i D_i$$

$$\overrightarrow{\mathcal{S}_{MomIi}} \cdot \overrightarrow{y_b} = \alpha\gamma_i \left(\frac{B_i + C_i - A_i}{2} \right) - \alpha\alpha_i E_i + \beta\gamma_i F_i - \beta\alpha_i D_i + \gamma\gamma_i E_i - \gamma\alpha_i \left(\frac{A_i + B_i - C_i}{2} \right)$$

$$\overrightarrow{\mathcal{S}_{MomIi}} \cdot \overrightarrow{z_b} = \alpha\alpha_i F_i - \alpha\beta_i \left(\frac{B_i + C_i - A_i}{2} \right) + \beta\alpha_i \left(\frac{A_i + C_i - B_i}{2} \right) - \beta\beta_i F_i + \gamma\alpha_i D_i - \gamma\beta_i E_i$$

where we denote $\overrightarrow{A(G_i, S_i/\mathcal{R}_b)}$ the acceleration of the center of mass G_i belonging to the body S_i with respect to the reference frame $\mathcal{R}_b$, (α, β, γ) the coordinates of the instananeous rotation vector $\overrightarrow{\Omega_0^b}$ expressed in $\mathcal{R}_0$ and $(\alpha_i, \beta_i, \gamma_i)$ the coordinates of the instananeous rotation vector $\overrightarrow{\Omega_0^i}$ expressed in $\mathcal{R}_0$.

As a result, once projected on the axes of the reference frame $\mathcal{R}_0$, the system to be solved can be written

as equation 5 :

$$
\overbrace{
\begin{bmatrix}
1 & 0 & 0 & 0 & z_G & -y_G \\
0 & 1 & 0 & -z_G & 0 & x_G \\
0 & 0 & 1 & y_G & -x_G & 0 \\
0 & -z_G & y_G & \frac{A_S}{M_S} & \frac{-F_S}{M_S} & \frac{-E_S}{M_S} \\
z_G & 0 & -x_G & \frac{-F_S}{M_S} & \frac{B_S}{M_S} & \frac{-D_S}{M_S} \\
-y_G & x_G & 0 & \frac{-E_S}{M_S} & \frac{-D_S}{M_S} & \frac{C_S}{M_S}
\end{bmatrix}}^{\mathbb{A}}
\frac{d}{dt}
\overbrace{
\begin{bmatrix}
\dot{x} \\ \dot{y} \\ \dot{z} \\ \alpha \\ \beta \\ \gamma
\end{bmatrix}}^{\dot{\boldsymbol{X}}_\Omega}
=
\frac{1}{M_S}
\overbrace{
\begin{bmatrix}
\vec{\mathcal{T}} \cdot \vec{x_0} - \overrightarrow{S_{Res}} \cdot \vec{x_0} \\
\vec{\mathcal{T}} \cdot \vec{y_0} - \overrightarrow{S_{Res}} \cdot \vec{y_0} \\
\vec{\mathcal{T}} \cdot \vec{z_0} - \overrightarrow{S_{Res}} \cdot \vec{z_0} \\
\overrightarrow{\mathcal{M}_{O_b}} \cdot \vec{x_0} - \vec{S_I} \cdot \vec{x_0} - \overrightarrow{S_{Mom}} \cdot \vec{x_0} \\
\overrightarrow{\mathcal{M}_{O_b}} \cdot \vec{y_0} - \vec{S_I} \cdot \vec{y_0} - \overrightarrow{S_{Mom}} \cdot \vec{y_0} \\
\overrightarrow{\mathcal{M}_{O_b}} \cdot \vec{z_0} - \vec{S_I} \cdot \vec{z_0} - \overrightarrow{S_{Mom}} \cdot \vec{z_0}
\end{bmatrix}}^{\boldsymbol{B}}
\tag{5}
$$

where we define :
— (A_S, B_S, C_S) and (D_S, E_S, F_S) the moments and the products inertia matrix for the global system S expressed at the point O_b,
— (x_G, y_G, z_G) the coordinates of the vector $\overrightarrow{O_bG}$ expressed in the basis β_0,
— (x, y, z) the coordinates of the vector $\overrightarrow{O_0O_b}$ in β_0 and $(\dot{x}, \dot{y}, \dot{z})$ the coordinates of the vector $\overrightarrow{V(O_b/\mathcal{R}_0)}$ expressed in β_0,

and where we recall the expression of the components of $\vec{S_I}$ already developed in [11] :

$$
\begin{aligned}
\vec{S_I} \cdot \vec{x_b} &= \alpha\,\gamma\,F_S - \alpha\,\beta\,E_S + (\gamma^2 - \beta^2)\,D_S + \beta\,\gamma\,(C_S - B_S) \\
\vec{S_I} \cdot \vec{y_b} &= \alpha\,\beta\,D_S - \beta\,\gamma\,F_S + (\alpha^2 - \gamma^2)\,E_S + \alpha\,\gamma\,(A_S - C_S) \\
\vec{S_I} \cdot \vec{z_b} &= \beta\,\gamma\,E_S - \alpha\,\gamma\,D_S + (\beta^2 - \alpha^2)\,F_S + \alpha\,\beta\,(B_S - A_S)
\end{aligned}
\tag{6}
$$

Since the Cardan angles are the variables used to parameterize the orientation, we compute a transformation matrix $\mathbb{C}$ such that $\dot{\boldsymbol{X}}_\Omega = \mathbb{C}\dot{\boldsymbol{X}}_C$, where $\dot{\boldsymbol{X}}_C^T = [\dot{x}, \dot{y}, \dot{z}, \dot{\phi}, \dot{\theta}, \dot{\psi}]$.

Finally, the system to be solved is described as equation (7) :

$$
\mathbb{A}\left[\mathbb{C}\frac{d}{dt}\left(\dot{\boldsymbol{X}}_C\right) + \dot{\mathbb{C}}\dot{\boldsymbol{X}}_C\right] = \boldsymbol{B}
\tag{7}
$$

The temporal discretization has been given to the classical second order BDF2 (Backward Difference Formulae) scheme, which is the one used for the fluid solver, see section 4.1. Some verification procedures have been done to check the implementation such as the reproduction of a gyroscopic motion, and some simple 1-DOF analytical motions too. It was also checked that starting from an initial state at rest, the initial position and orientation of the boat are recovered after moving the different bodies of the system without any external force.

3   Modelling of the fluid flows

In rowing, two kind of fluid flows are involved, around the hull and the blades. The first one is not so easy to investigate. As a matter of fact, the unsteadiness of the propulsion associated to the motion of the athlete with respect to his hull leads to a great oscillating surge motion coupled with non-negligeable pitch and heave secondary motions. It makes it singular regarding the flow around hulls in calm water in

hydrodynamics. Friction resistance is the main part of the total resistance for such a hull. But the possible roughness effect of the hull and the unsteadiness of the turbulent boundary layer at the wall makes the modeling more tricky than it can be thought. However, the flow around the oar blade is definively more complex to handle : the blade moves with a complex 6 DOF motion close to the free surface, leading to an unsteady flow with a very complex shape of free surface varying in time and including breakup. It also involves fluid-structure interaction through the flexibility of the shaft. It easily explains the limits of simplified models often used in the literature ([3, 30]) and justify the use of a high-fidelity model, even if it requires far more computational power.

3.1   Need for high-fidelity CFD model

Simplified models can be useful to initialize the boat dynamics to impose as a starting point for the resolution of high-fidelity model. However, even if they could be improved in the future, we are now convinced that they will never take care into account all the subtle interactions which appear during the propulsive phase, especially during the catch phase, which is essential to the propulive force generation of the whole stroke. Some years ago, experimental research works were done to try to characterize the flow and deduce an accurate simplified model ([2, 3]). Then, numerical simulations have been investigated for its capabilities to deal more easily with complex motions, and to replace measurement by numerical result to improve the calibration of a simplified model ([12, 13, 21]). However, in consideration of the great number of parameters to define accurately the motion of the blade and the physics of the flow, the building of an accurate surrogate model based on a response surface model for the temporal fluid force actin on the blade appears unaffordable. Finally, it was decided to directly coupled the high-fidelity model to power the fluid force of the global mechanical system, without any compromise in accuracy ([22]). This choice is all the more sustainable that the increase of the HPC resources can limit nowadays the physical response time of such a configuration in less than a day.

3.2   ISIS-CFD solver

ISIS-CFD is available as a part of the FINE^{TM}/Marine computing suite which is dedicated to marine applications. This is an incompressible unsteady Reynolds-averaged Navier–Stokes (RANS) solver developed by ECN-CNRS ([19]). This solver is based on a cell-centred unstructured finite-volume method. Pressure–velocity coupling is obtained through a Rhie & Chow SIMPLE-type method. Free-surface flow is addressed with an interface capturing method, by solving a convection equation for the volume fraction of water, which is discretised with specific compressive discretisation schemes ([18]). An Arbitrary Lagrangian Eulerian (ALE) formulation is used to take into account modification of the fluid spatial domain ([12]). It is associated with robust and fast grid deformation techniques ([11]). The temporal discretisation scheme is the Backward Difference Formula of order 2 (BDF2) when dealing with unsteady configurations. For each time step, an inner loop (denoted by non-linear loop) associated to a Picard linearisation is used to solve the non-linearities of the system. The code is fully parallel using the MPI (Message Passing Interface) protocol. An automatic adaptive grid refinement technique ([29]) as well as overlapping grid technology are also included.

4   Co-simulation between ISIS-CFD and SPRing

Co-simulation, which involves codes coupling, is the most popular technique in an industrial context to deal with multi-physics applications. This is mainly due to its modular nature and the use of specialized

solvers which have the ability to integrate the most advanced numerical techniques and physical models in each scientific field. Here, a dedicated tool modeling the global system boat-rower(s)-oars (SPRing, see section 2) is associated to a general purpose CFD solver for incompressible and turbulent flow (ISIS-CFD) to provide an accurate evaluation of the fluid forces acting on the system to reach an high-fidelity model.

The data exchange between the two codes is driven by a TCP/IP socket-based protocol, using the ZeroMQ distributed message library ([1]). This communication interface enables to easily exchange data between different programming language such as Fortran and Python in the present case.

However, specific attention has to be paid to coupling strategies to be both accurate and stable.

4.1   Coupling algorithm and stabilization

In the present configuration, two separated fluid-structure interactions are solved. The first one concerns the fluid forces acting on the hull and on the blades computed by the CFD solver which interacts with the dynamics of the system, i.e. the dynamics of the hull. The second one is related to the flexibility of the shaft which depends on the fluid force action on the blade. Both are submitted to large added mass effects and then are subjected to numerical instabilities.

To tackle this issue, an internal implicit coupling is used in conjunction with an artificial added-mass method ([7, 11, 32, 33]) The resolution of the dynamic of the global system is then solved at each non-linear iteration of the fluid solver. New positions of the hull and of the blades due to the flexibility of the shaft are updated and taken into account to progress in both the convergence of the fluid flow and the convergence of the FSI problems. A simplified coupling diagram is presented in figure 3.
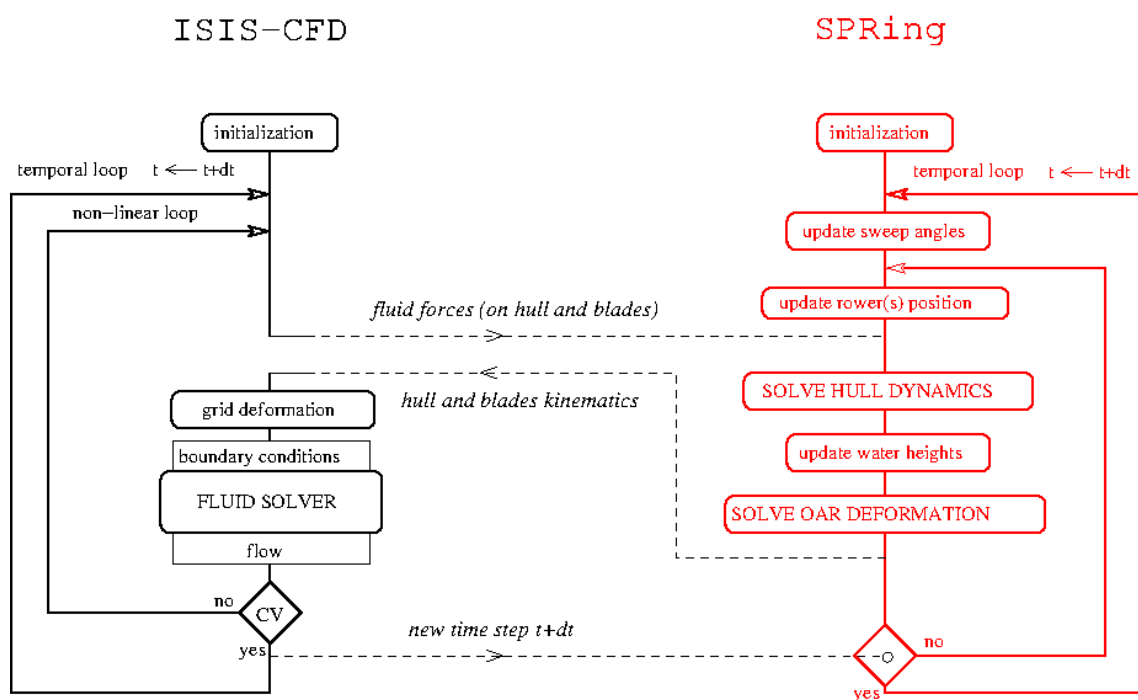

FIGURE 3 – Coupling diagram

Considering the discrete timeline as described in figure 4, and the BDF2 scheme expressed in equation (8), the discrete operator to solve the hull dynamics (equation (9)) is deduced from equation (7),

where k refers to the index of the non-linear loop of the fluid solver. In the present case, the added-mass operator $\tilde{\mathbb{M}}_a$ is evaluated in the CFD solver itself using the same method as described in [33].
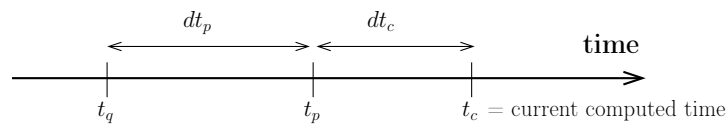

FIGURE 4 – Discrete timeline

$$\left.\frac{df}{dt}\right|_c = e_c\,f(t_c) + e_p\,f(t_p) + e_q\,f(t_q)$$

$$\text{with } e_c = \frac{2dt_c + dt_p}{dt_c\,(dt_c + dt_p)},\ e_p = -\frac{dt_c + dt_p}{dt_c dt_p},\ e_c = \frac{dt_c}{dt_p\,(dt_c + dt_p)} \tag{8}$$

$$\left[\mathbb{A}_c^{k-1} + \frac{\tilde{\mathbb{M}}_a}{M_S}\right]\left(\mathbb{C}_c^{k-1}e_c + \dot{\mathbb{C}}_c^{k-1}\right)\dot{\boldsymbol{X}}_{Cc}^k = \boldsymbol{B}_c^{k-1}$$

$$- \left[\mathbb{A}_c^{k-1} + \frac{\tilde{\mathbb{M}}_a}{M_S}\right]\mathbb{C}_c^{k-1}\left(e_p\dot{\boldsymbol{X}}_{Cp} + e_q\dot{\boldsymbol{X}}_{Cq}\right) \tag{9}$$

$$+ \frac{\tilde{\mathbb{M}}_a}{M_S}\frac{d}{dt}\left(\mathbb{C}_c^{k-1}\dot{\boldsymbol{X}}_{Cc}^{k-1}\right)$$

The structural model of the oar to take into account the flexibility of the shaft is the complete model described in [22], where the linear and angular stiffness coefficients are supposed to be measured with respect to the deformed oarlock line (line tangent to the deformed shaft at the oarlock location) : contrary to the specific device built to test real oar in the towing tank which was used in [22] where the rotating arm imposed the angular motion of the non-deformed oarlock line, in-situ measurements give the sweep angle including the rotation of the oarlock induced by the deformation of the shaft, see figure 5. As it is detailed in [22], a quasi-static approach with an added-mass stabilization is used with an update of the added-mass operator given by the CFD solver.
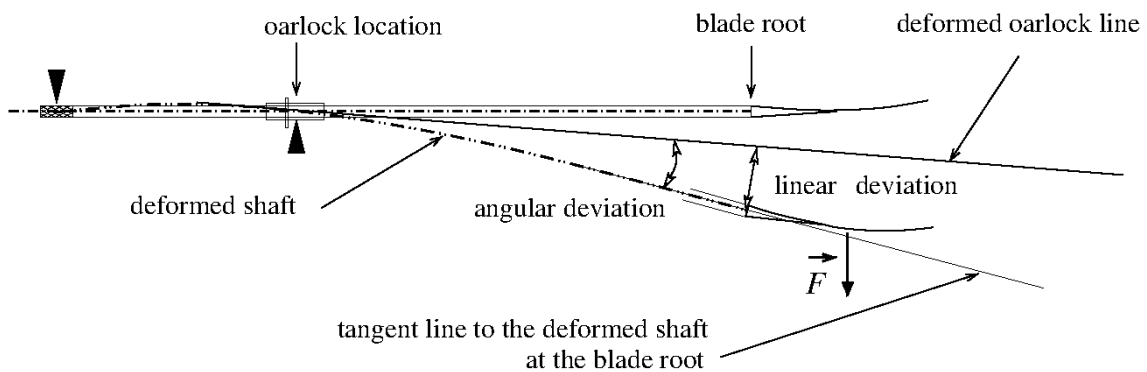

FIGURE 5 – Linear and angular deviation with respect to the deformed oarlock line

4.2 Control of the system and simulation

An initial phase starts with a speed-up of the hull using an imposed forward velocity ramp up to a guess velocity while keeping solving heave and pitch. In the meanwhile, the rower moves from his initial position (sweep angle 90 deg, see figure 6) to the catch phase with a smooth kinematic connection at the configuration when the height of the blade reaches its maximum value. This connection is done at the time when the whole resolution of the dynamics starts.
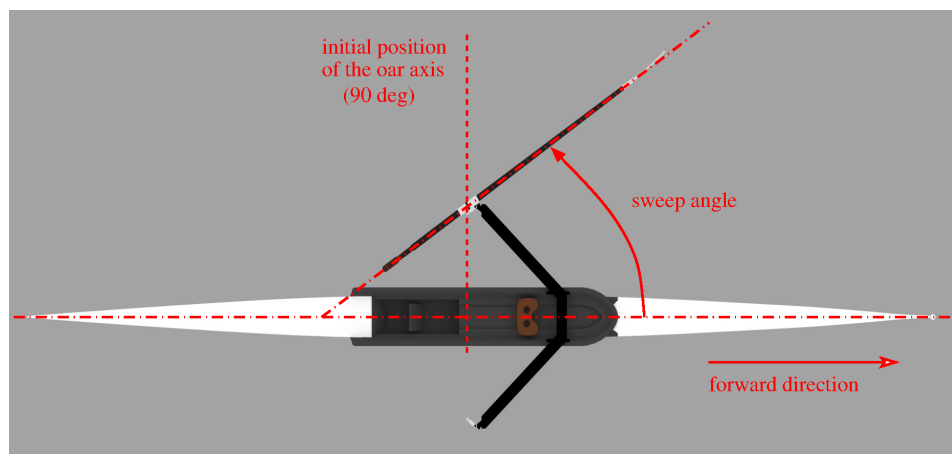

FIGURE 6 – Definition of the sweep angle

As discussed in section 2, it was decided to drive the rower through the temporal evolution of the sweep angle, instead of driving the different joins which composes the rower model. This input data, which can be extracted from in-situ measurements, only sets the longitudinal positions of the hands of the rower, but not his global body with respect to the boat. As a consequence, additional information is required to fully describe the technical gesture. Without going into too much detail, the motion laws of the different body parts (legs,spine and arms) are computed from percentage rates, which evolve according to the sweep angle. The body position is then computed successively by moving the differents body parts for a given modification of the sweep angle according to these ratio. Some additional features (spine curvature, detachment of the heel close to the catch phase,...) have also be implemented to enrich the possible kinematics of the rower. To complete the control of the system, the vertical position of the blades, which corresponds to the vertical position of the rower's hands, has to be driven. Here again, it was decided to specify the height of the blade root with respect to the water (denoted as water height). Here again, this choice is rather unusual since this data depends on the boat attitude. As a result, the angle of the oar with respect to the horizontal plane has to be dynamically computed. However, it appears to be the more judicious choice since it corresponds to what is controlled by the rower and what it is looked at by the coaches. It is thus in line with the objective to have the most operational tool.

Other input data as density and geometry of each members of the rower are mainly based on the work described in [15, 31] . A first simulation has been carried out using a quite coarse mesh of 2.3 million cells, based on measurements with a rower who followed the project-based specialisation "PariSci2024" (see figure 7). Advanced numerical methods, such as overset grids, adaptive grid refinement, mesh deformation, have to be used to carry out such a configuration.

Another important aspect of the project concerns the realistic rendering of the simulation (figure 8). It has been developed using the open-source Blender software. This tool is important as a communication facility with coaches, but also to easier confront the reality with the simulation. Once synchronised with
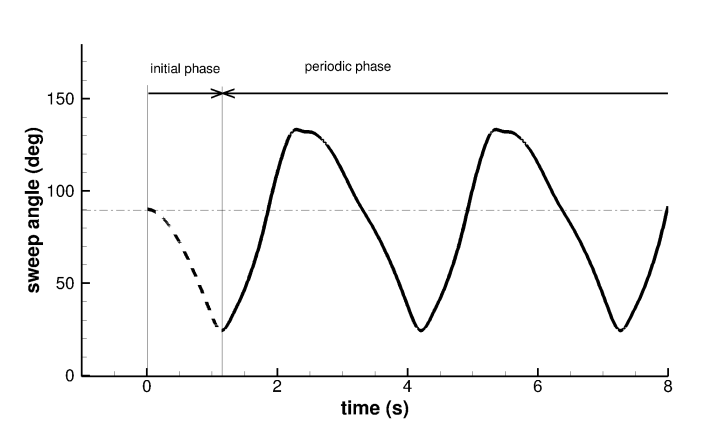
FIGURE 7 – Imposed sweep angle as a function of time

specific outputs (acceleration, incident velocity around the blade,...), the physical analysis will be greatly facilitated too.
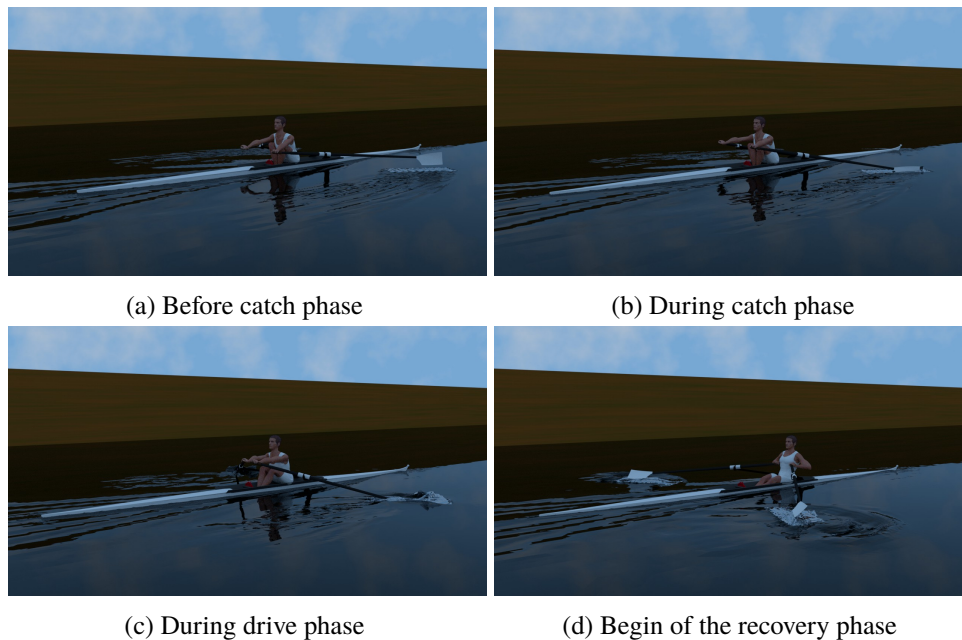

(a) Before catch phase

(b) During catch phase

(c) During drive phase

(d) Begin of the recovery phase

FIGURE 8 – Realistic rendering of the simulation

5   Conclusion and perspectives

It is demonstrated in this work the proof of concept of a high-fidelity model of the system boat-rower(s)-oars, designed as a future tool to analyse and to serve performance in rowing. Before playing this role, an extensive step of validation for these coupled simulations needs to be investigated using in-situ measurement. The main issue concerns the incomplete set of measured data available to drive the simulation. As an example, until now, no experimental device is able to measure accurately the height of the blade with respect to the water. As a result, until a better solution is found, video analysis is going to be used to calibrate this input kinematics. This validation step is fondamental because Science can bring a new right insight on sport performance, only if the modelization lives up to the expectations in term of accuracy so that the physical analysis of the phenomena can be trustingly carried out. In parallel of that, more

advanced mechanical analysis (loads on human joints, power consumption, efficiency,...) is planned to benefit from all the data which are computed. At term, such tool targets to bring objective and unbiased criteria for questions which have only empirical answers up to now .

Acknowlegment

Références

[1] F. Akgul. *ZeroMQ*. Packt Publishing, 2013. ISBN 178216104X, 9781782161042.

[2] S. Barré. *Etude expérimentale des systèmes de propulsion instationnaire. Application aux palettes d'aviron*. PhD thesis, Université de Nantes, 1998.

[3] S. Barré and J. Kobus. Comparison between common models of forces on oar blades and forces measured by towing tank tests. *Proceedings of the Institution of Mechanical Engineers, Part P : Journal of Sports Engineering and Technology*, 224(1) :37–50, 2010.

[4] M. Brearley, N. de Mestre, and D. Watson. Modelling the rowing stroke in racing shells. *The Mathematical Gazette*, pages 389–404, 1998.

[5] D. Cabrera, A. Ruina, and V. Kleshnev. A simple 1+ dimensional model of rowing mimics observed forces and motions. *Human movement science*, 25(2) :192–220, Febuary 2006. PariSci2024.

[6] N. Caplan and T. Gardner. Modeling the Influence of Crew Movement on Boat Velocity Fluctuations during the Rowing Stroke. *International Journal of Sports Science and Engineering*, 1(3) : 165–176, 2007.

[7] M. Durand, A. Leroyer, C. Lothodé, F. Hauville, M. Visonneau, R. Floch, and L. Guillaume. {FSI} investigation on stability of downwind sails with an automatic dynamic trimming. *Ocean Engineering*, 90(0) :129–139, 2014. ISSN 0029-8018. doi : http ://dx.doi.org/10.1016/j.oceaneng.2014.09.021. URL `http://www.sciencedirect.com/science/article/pii/S002980181400345X`.

[8] L. Formaggia, E. Miglio, A. Mola, and A. Montano. A model for the dynamics of rowing boats. *International Journal for Numerical Methods in Fluids*, 61(2) :119–143, 2009. ISSN 1097-0363.

[9] L. Formaggia, A. Mola, N. Parolini, and M. Pischiutta. A three-dimensional model for the dynamics and hydrodynamics of rowing boats. *Proceedings of the Institution of Mechanical Engineers, Part P : Journal of Sports Engineering and Technology*, pages 1–11, 2009.

[10] A. Hay, A. Leroyer, and M. Visonneau. H-adaptive Navier–Stokes simulations of free-surface flows around moving bodies. *Journal of Marine Science and Technology*, 11(1) :1–18, 2006. ISSN 0948-4280. 2006 JASNAOE Paper Award, Japanese Society of Naval Architecture and Ocean Engineering.

[11] A. Leroyer and M. Visonneau. Numerical methods for RANSE simulations of a self-propelled fish-like body. *Journal of Fluids and Structures*, 20(7) :975–991, 2005. ISSN 0889-9746.

[12] A. Leroyer, S. Barré, J. Kobus, and M. Visonneau. Experimental and numerical investigations of the flow around an oar blade. *Journal of Marine Science and Technology*, 13(1) :1–15, 2008.

[13] A. Leroyer, S. Barré, J. Kobus, and M. Visonneau. Influence of free surface, unsteadiness and viscous effects on oar blade hydrodynamic loads. *Journal of Sports Sciences*, 28(12) :1287–1298, 2010.

[14] A. Leroyer, P. Queutey, and R. Duvigneau. Vers l'optimisation de la performance en kayak par la simulation numérique. In *15 ième Journée de l'hydrodynamique*, 2015.

[15] P. D. Leva. Adjustments to zatsiorsky-seluyanov's segment inertia parameters. *Journal of Biomechanics*, 29(9) :1223 – 1230, 1996. ISSN 0021-9290. doi : https ://doi.org/10.1016/0021-9290(95)00178-6. URL `http://www.sciencedirect.com/science/article/pii/0021929095001786`.

[16] R. Pettersson, A. Nordmark, and A. Eriksson. Simulation of rowing in an optimization context. *Multibody System Dynamics*, 32 :337–356, 2014. multi-body dynamics, rowing.

[17] D. Pope. On the dynamics of men and boats and oars. *Mechanics and Sport*, 4 :113–130, 1973.

[18] P. Queutey and M. Visonneau. An interface capturing method for free-surface hydrodynamic flows. *Computers & fluids*, 36(9) :1481–1510, 2007. ISSN 0045-7930.

[19] P. Queutey, G. Deng, J. Wackers, E. Guilmineau, A. Leroyer, and M. Visonneau. Sliding grids and adaptive grid refinement for rans simulation of ship-propeller interaction. *Ship Technology Research*, 59(2) :44–58, April 2012.

[20] Y. Robert. *Simulation numérique et modélisation d'écoulements tridimensionnels instationnaires à surface libre. Application au système bateau-avirons-rameur.* PhD thesis, Centrale Nantes, 2017.

[21] Y. Robert, A. Leroyer, S. Barré, F. Rongère, P. Queutey, and M. Visonneau. Fluid mechanics in rowing : The case of the flow around the blades. *Procedia Engineering*, 72 :744–749, 2014. doi : https ://doi.org/10.1016/j.proeng.2014.06.126.

[22] Y. Robert, A. Leroyer, S. Barré, P. Queutey, and M. Visonneau. Validation of cfd simulations of the flow around a full-scale rowing blade with realistic kinematics. *Journal of Marine Science and Technology*, 2018. doi : https ://doi.org/10.1007/s00773-018-0610-y.

[23] F. Rongère. *Simulation dynamique des systèmes Bateau-Avirons-Rameur (s).* PhD thesis, Ecole Centrale de Nantes, 2011.

[24] F. Rongère, W. Khalil, and J.-M. Kobus. Dynamic modeling and simulation of rowing with a robotics formalism. In *Methods and Models in Automation and Robotics (MMAR), 2011 16th International Conference on*, pages 260 –265, aug. 2011. doi : 10.1109/MMAR.2011.6031355.

[25] B. Sanderson and W. Martindale. Towards optimizing rowing technique. *Medicine & Science in Sports & Exercise*, 18(4) :454–468, 1986.

[26] S. Serveto, S. Barré, J. Kobus, and J. Mariot. A three-dimensional model of the boat-oars-rower system using ADAMS and LifeMOD commercial software. *Proceedings of the Institution of Mechanical Engineers, Part P : Journal of Sports Engineering and Technology*, pages 1–14, 2009.

[27] A. Sliasas and S. Tullis. The dynamic flow behaviour of an oar blade in motion using a hydrodynamics-based shell-velocity-coupled model of a rowing stroke. *Proceedings of the Institution of Mechanical Engineers, Part P : Journal of Sports Engineering and Technology*, pages 1–16, 2009.

[28] A. Sliasas and S. Tullis. A hydrodynamics-based model of a rowing stroke simulating effects of drag and lift on oar blade efficiency for various cant angles. *Procedia Engineering*, 2(2) :2857–2862, 2010. ISSN 1877-7058.

[29] J. Wackers, G. Deng, A. Leroyer, P. Queutey, and M. Visonneau. Adaptive grid refinement for hydrodynamic flows. *Computers & Fluids*, 55(0) :85–100, 2012. ISSN 0045-7930. doi : 10.1016/j.compfluid.2011.11.004. URL http://www.sciencedirect.com/science/article/pii/S0045793011003392.

[30] J. Wellicome. Some hydrodynamic aspects of rowing. In *Rowing : A Scientific Approach, A Symposium*, 1967.

[31] M. Yeadon. The simulation of aerial movement—ii. a mathematical inertia model of the human body. *Journal of Biomechanics*, 23(1) :67 – 74, 1990. ISSN 0021-9290. doi : https ://doi.org/10.1016/0021-9290(90)90370-I. URL http://www.sciencedirect.com/science/article/pii/002192909090370I.

[32] C. Yvin. *Interaction fluide-structure pour des configurations multi-corps. Applications aux liaisons complexes, lois de commande d'actionneur et systèmes souples dans le domaine maritime.* PhD thesis, Ecole Centrale de Nantes, 2014.

[33] C. Yvin, A. Leroyer, M. Visonneau, and P. Queutey. Added mass evaluation with a finite-volume solver for applications in fluid–structure interaction problems solved with co-simulation. *Journal of Fluids and Structures*, 81 :528–546, 2018.